Environ. Sci. Technol. **1998**, *32,* 1727−1733

Theoretical and Experimental Analysis of Peeper Equilibration Dynamics

IAN T. WEBSTER,*,† PETER R. TEASDALE,‡,§ AND NICOLA J. GRIGG†

CSIRO Land & Water, GPO Box 1666, Canberra, ACT 2601, Australia, Centre for Advanced Analytical Chemistry, CSIRO, PMB 7, Bangor, NSW 2234, Australia

Peepers are multichambered equilibrium dialyzers placed within sediments to collect porewater samples. We developed computer models to study the equilibration dynamics of a vial peeper design. One model simulated the concentration distributions and dynamic behavior of solute within the peeper cell itself, and another simulated the equilibration of peepers placed within sediments. The first model, together with laboratory experiments, demonstrated that convection arising within peeper cells placed in saline sediments would ensure rapid mixing of the contents of the cells. The predictions of equilibration behavior made by the second model for four chemical species (K, Na, Ca, and Sr) generally compared well with the results of laboratory experiments. These results showed that peeper equilibration was limited almost wholly by solute diffusion through the sediments and demonstrated the importance of peeper dimensions and solute diffusivities for equilibration times.

Introduction

Peepers are multichambered equilibrium dialyzers used to sample sediment pore waters in situ. They comprise a semipermeable membrane that lies across the openings of a series of cells in a plastic support material. These cells contain a receiver solution (typically deionized, deoxygenated water) and provide multiple porewater samples at a spatial resolution typically on a centimeter scale. They are left in situ for a period of time deemed sufficient to allow diffusion to transport dissolved constituents across the membrane, bringing the receiver solution to equilibrium with the porewaters. It is important to estimate the equilibration time for species of interest or, more practically, to estimate the extent of equilibration attained for a given deployment time.

Hesslein (*1*), in his first description of the sampling technique, measured the equilibration characteristics in water and concluded that the device must be left in situ much longer than indicated by these measurements: "in sediments the interstitial water directly adjacent to the membrane becomes depleted of dissolved constituents by flux into the compartment and additional time must be allowed for this zone to be replenished by flux from the surrounding interstitial water." Carignan (*2*) recognized that factors that limited peeper equilibration in sediments were species diffusivity, solid-phase adsorption, temperature, and porosity. For porosities in recently deposited sediments, he suggested equilibration times of 15−20 days for Hesslein-type peepers based upon measurements in the field. Peeper deployment periods have typically been about 2 weeks (*3*−*5*).

Adler (*6*) used peepers to measure porewater solute diffusivities by comparing experimental data to a numerical model of diffusive transport through the sediment pores and peeper cell. He commented that such an approach is limited by the lack of knowledge about the controlling transport processes within the cell and across the membrane. Harper et al. (*7*) employed a two-dimensional diffusion model to investigate the equilibration dynamics of Hesslein-type peepers. Three cases were considered: well-buffered porewater due to desorption or dissolution; diffusion only in the sediment, with no resupply; and partial resupply from the solid phase.

Our study employed a two-dimensional model to investigate the second scenario in ref *7*, which assumed no resupply from the solid phase. We investigated whether the results of a series of peeper equilibration experiments could be well described using such a peeper model. The experiments involved vial peepers of three different cell sizes and four chemical species (K, Na, Ca, Sr). The results demonstrated the importance of cell size and of the diffusivity of the diffusing chemical species for determining equilibration times. A factor of potential importance to peeper equilibration, particularly for peeper cells of relatively large dimension (>10 mm), is the effect of incomplete mixing of solute within the cell itself. We also investigated the effects of convection on cell mixing. Convection is initiated when a cell is filled with deionized water and deployed in pore waters containing significant ionic concentration. We have developed a criterion that allows investigators to determine when incomplete cell mixing is likely to become a major consideration for peeper equilibration.

Experimental Methods

The peeper used in our experiments comprised a polyethylene vial (Canberra Packard) and 0.45 μm polysulfone membrane (Gelman HT450). The design factor, F, is defined as

$$F = V/A \qquad (1)$$

where V is the vial volume and A is the area of the membrane. Series of vial peepers have been mounted on rods in order to obtain profiles of species concentrations in sediments or in saturated soils (*8, 9*).

The vial peepers in experiment 1 had a length of 53 mm and a uniform diameter of 22 mm (design factor 53 mm), and the membrane was held in place with two tight "O"-rings. For experiment 2, vial peepers having design factors of 15, 57, and 99 mm were employed. The vials used were of 57 mm length, 25 mm maximum diameter, and volume 25.2 mL (design factor 99 mm). The design factor for a vial of uniform diameter is simply the length of the vial, but the vials in experiment 2 did not have a uniform cross-sectional area along their lengths (Figure 1a). For the vial having a 57-mm design factor, plastic strips were placed inside a normal vial to reduce its volume. A vial with a 15-mm design factor was obtained by compressing a normal vial within a

* To whom correspondence should be addressed. E-mail: Ian.Webster@cbr.clw.csiro.au; telephone: +61 2 6246 5581; fax: +61 2 6246 5560.

† CSIRO Land & Water.

‡ Centre for Advanced Analytical Chemistry.

§ Present address: Environmental Science, Institute of Environmental and Natural Sciences, Lancaster University, Lancaster LA1 4YQ, U.K.

S0013-936X(97)00815-8 CCC: $15.00
Published on Web 04/08/1998

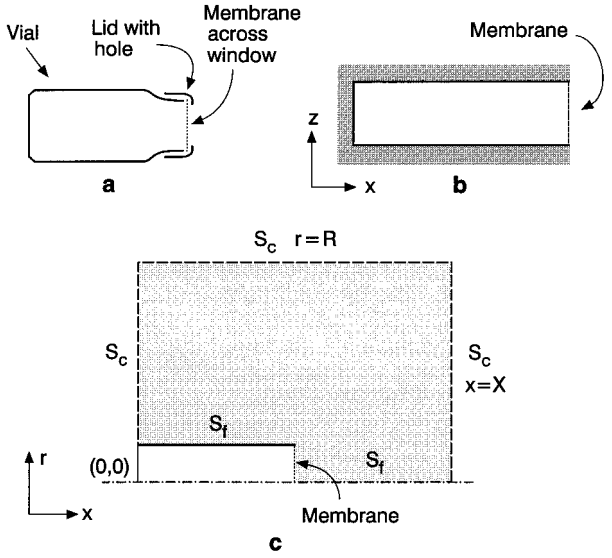

FIGURE 1. (a) Schematic of the vial peeper used in the experiments. (b) Domain for the computer simulation of in-cell equilibration. (c) Domain for the computer simulation of in-sediment equilibration.

glass collar on a hot plate, which reduced its volume to 3.8 mL. For these vials, the membrane was held in place by screwing on a lid with a large hole cut in it (Figure 1a). The membrane permeation speed k^m was determined by measuring the flux of bromide across a membrane separating two known volumes.

Experiment 1: Peeper Equilibration—Water. This experiment involved no sediment and was designed to determine the sensitivity of peeper equilibration to cell orientation. Twenty-four vial peepers were filled with distilled water and placed in a 15-L tank filled with a 35 g L^{-1} salt (99% NaCl) solution and a bromide tracer. One set of vials was mounted vertically with their windows facing up (samples 1−8); another set was mounted horizontally with its windows facing sideways (samples 9−16), and the third set had its vial windows facing directly downward (samples 17−24). Vials were removed from each of the three orientations at known times, and their contents were analyzed for bromide concentration using flow injection analysis (FIA), which determines the bromide concentration colorimetrically using the phenol red method (*10*).

Experiment 2: Peeper Equilibration—Sediment. Sediment for the time series experiments was collected from a site in the Georges River, Sydney, which is subject to inundation by seawater. In the laboratory, the sediment was placed in a 40-L bin, mixed well with a shovel, overlain with water collected from the same site on the same day, and allowed to sit for about 48 h.

The materials used to assemble the vials were deoxygenated in a nitrogen atmosphere for up to 5 weeks. This procedure ensured that oxygen release did not influence the equilibration rates by causing metal oxyhydroxide deposition (*11*). Each vial was filled with deoxygenated, deionized water. The vials were placed in the sediment at a depth greater than 50 mm in order to conduct the equilibration under anoxic conditions, at least 50 mm from one another, and covered over with sediment. The middle-sized and largest vials were placed in one bin; the smallest peepers were placed in a second bin. An individual vial was allowed to equilibrate with the sediment porewaters for a predetermined number of days before being removed and sampled. The samples were then acidified to about pH 1.5 with concentrated nitric acid (Normatom) prior to their analysis for total K, Na, Ca, and Sr by inductively coupled plasma atomic emission spectroscopy (ICPAES) (Spectro Analytical Instruments). Each measurement was performed in triplicate, and a standard deviation of less than 10% (usually <5%) was obtained for each sample.

Independent measurements of the porewater concentrations were obtained on sediment core sections, taken from a depth greater than 50 mm, collected from each sediment bin. These samples were centrifuged and then filtered through a 0.45-μm membrane before analysis. The results were used for the independently measured pore water values (C_0) in the calculations described later. Triplicate measurements gave a sediment porosity of 0.44 ± 0.02.

Modeling Methods

In-Cell Equilibration Dynamics. At the beginning of experiment 1, the vials were filled with distilled water, covered with a membrane, and immersed in water having a constant salinity. As the experiments proceeded, salt diffused across the membrane and caused the salinity of the water near the membrane on the inside of the cell to increase. We expected that, for the upward and sideway facing membrane orientations, this denser saline water near the membrane would tend to flow away from the membrane. Thus, equilibration within the vial would depend on convective as well as diffusive processes. We constructed a numerical model to test this assumption. The model needed to be able to simulate the salt and bromide distributions in the vial and the in-cell velocity field generated by the salt distribution.

Although the peeper cell has a cylindrical shape, we modeled the in-cell equilibration dynamics using a two-dimensional model for simplicity. A two-dimensional model would describe the gross features of solute diffusion and of the flow within the vial. The long vial and lateral coordinates were x and z, respectively (Figure 1b). The velocity dynamics within the cell were modeled using a vorticity-stream function approach (*12*). The flow within the cell was assumed to be of low Reynolds number; that is, viscous forces were assumed to dominate.

We used a standard finite difference technique (*12*) to solve the vorticity equation [derived from the low Reynolds number Navier−Stokes equation (*13*) with the Boussinesq assumption (*14*)] and the two-dimensional advection−diffusion equation within a peeper cell. We assumed variations from the initial density were linearly related to the salinity.

The model stepped forward in time from initial conditions of zero vorticity and salinity. The boundary conditions assumed that the tangential and normal flows across all the walls of the cell were zero and that the normal fluxes of salt across the three solid walls of the cell were also zero. The salt flux through the membrane was assumed to be equal to the product of the permeation speed, k^m, and the salt concentration difference across the membrane:

$$\text{flux} = k^m(s_{\text{out}} - s_{\text{in}}) \qquad (2)$$

where s_{in} and s_{out} are the concentrations on the inner and outer sides of the membrane, respectively. For the modeling of the in-cell equilibration dynamics, s_{in} is a function of position along the inner side of the membrane and s_{out} is held constant.

In-Sediment Equilibration Dynamics. We developed a numerical model to study the equilibration dynamics of the vial peeper design used in the experiments. We assumed that transport of solute through the sediments surrounding the peeper occurs by molecular diffusion through the pore spaces only. The bulk concentration of solute within the sediment is C_b which is taken to be a function of both position and time, t. The solute is assumed to be nonreactive with no resupply within the sediment through desorption or convection. This case is the "diffusive" case described by

Harper et al. (*7*) in their analysis of the equilibration of pore water samplers. If φ is the porosity of the sediment (assumed uniform), then the pore water concentration, C, is related to the bulk solute concentration by

$$C = C_b/\varphi \tag{3}$$

Assuming that diffusion of solute into the vial peeper is radially symmetric about the axis of the vial, the problem can be modeled in two dimensions employing cylindrical polar coordinates. In our model, the coordinate in the direction of the vial axis is x and the radial coordinate is r, as shown in Figure 1c. The equation for diffusion through the sediment surrounding the peeper is

$$\frac{\partial C_b}{\partial t} = \varphi D_s \frac{\partial^2 C}{\partial x^2} + \frac{\varphi D_s}{r} \frac{\partial}{\partial r} r \frac{\partial C}{\partial r} \tag{4}$$

where D_s is the diffusivity of the solute within the sediment. The molecular diffusivity within sediments is reduced from its value in free water D because diffusing molecules must follow a tortuous path around sediment grains (*15*). D_s is related to D by

$$D_s = D/\theta^2 \tag{5}$$

where θ is the tortuosity.

We applied a flux boundary condition equivalent to eq 2 at the membrane surface

$$\text{flux} = k^m(C - C_p) \text{ across membrane} \tag{6}$$

where C_p is the concentration in the peeper cell.

The flux of solute across the peeper window causes the mass of solute within the peeper cell to increase at the rate

$$V\frac{dC_p}{dt} = k^m A(\bar{C} - C_p) \tag{7}$$

where $\bar{C}$ is the average of the porewater concentration along the surface of the membrane window. We assumed also that the concentration within the peeper cell was spatially uniform, although this will not be the case. However, we estimate that the time scale for complete mixing within a vial placed on its side in a saline medium to be 4 h at worst and as little as 1 h, depending on the size of the vial. Since the time scale is much less than the time to diffuse solute through the sediment, the assumption of instantaneous mixing within the vial is a good one.

Zero flux boundary conditions were applied at surfaces S_f (Figure 1c). Along the surfaces S_c, the concentration was maintained at the initial (uniform) sediment concentration C_0 . The model stepped forward in time from initial conditions of $C = C_0$ and $C_p = 0$.

Results and Discussion

The membrane permeation speed was measured to be $k^m = 2.7 \times 10^{-3}$ mm s^{-1}. Accounting for experimental errors, the expected range of uncertainty is $2.6-3.1 \times 10^{-3}$ mm s^{-1}. The measurement of membrane permeation speed involved an analysis of the rate of equilibration of tracer concentration between two well-stirred containers separated by the dialysis membrane. The formation of diffusive boundary layers of unknown thickness on either side of the membrane would cause a resistance to exchange additional to that of the membrane and would lead to underestimation of the membrane permeation speed (*16*). We have used the measured permeation speed for further calculations, but the estimated uncertainty range in the speed includes the likely error due to diffusive boundary layer formation.

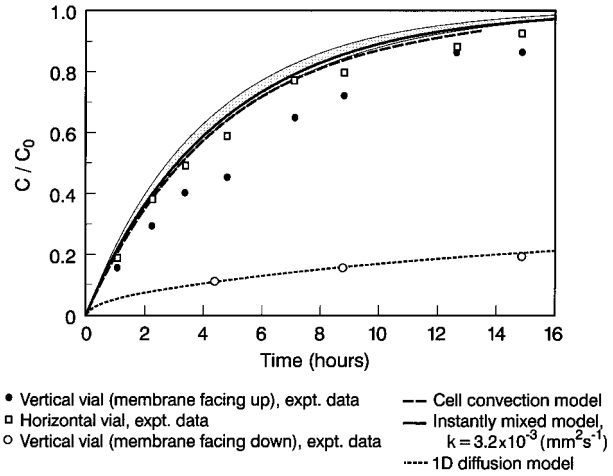

FIGURE 2. Comparison between measured and simulated vial bromide concentrations for the three vial orientations in experiment 1. Measurements from only three of the downward facing vials are included. Data from the remaining five vials continued to be well described by the diffusion-only model (the measurements were within 5% of the model prediction, with the exception of one point which was 6.6% lower than the model prediction), and after 60 h both model and experiment had reached approximately 40% equilibration. Also shown is the prediction from the instantly mixed model (eq 8). The shaded region represents the uncertainty in the membrane permeation speed measurement.

The membrane permeation speed is assumed to be directly proportional to the diffusivity of the species of interest. The diffusivity depends on the nature of the species involved, the temperature, and any electroneutrality conditions, as described by Li and Gregory (*17*). When we measured k^m, the sodium and bromide ions were the major ions in solution diffusing into freshwater; the maintenance of electroneutrality in the system requires that the sodium and bromide ions diffuse at the same rate. The bromide ions in experiment 1 were minor ions in seawater diffusing into freshwater. In this case, the bromide ions diffuse almost independently of other ions (*17*). Using the data and formulas presented by Li and Gregory (*17*), the membrane permeation speed used to model experiment 1 was adjusted to account for species diffusivity and temperature. The adjusted membrane permeation speed was calculated to be 3.2×10^{-3} mm s^{-1} (lying within a range of uncertainty of $3.1-3.6 \times 10^{-3}$ mm s^{-1}).

In-Cell Equilibration Dynamics. As expected, the vials that had their membrane facing down (samples 17−24) were the slowest to equilibrate in experiment 1. Even after 60 h the cells had achieved only 40% equilibration. Since the dense saltwater crossed into the vials along the bottom boundary, there was no tendency for haline convection to develop within the cells. To simulate this case, the numerical model was simplified to consider one-dimensional diffusion only within the cell. Figure 2 shows that the model prediction describes the measurements well. Vials 1−16 equilibrated much faster, exceeding 85% equilibration after 15 h; however, the vertical vials with the membranes facing up (samples 1−8) equilibrated more slowly than the horizontal vials (samples 9−16) (Figure 2).

If one assumes that the peeper cell is mixed instantaneously, that the concentration on the outside of the membrane is held constant at C_0, and that the only resistance to equilibration is permeation across the membrane, then the concentration within the cell increases as

$$C_p = C_0(1 - \exp(-k^m t/F)) \tag{8}$$

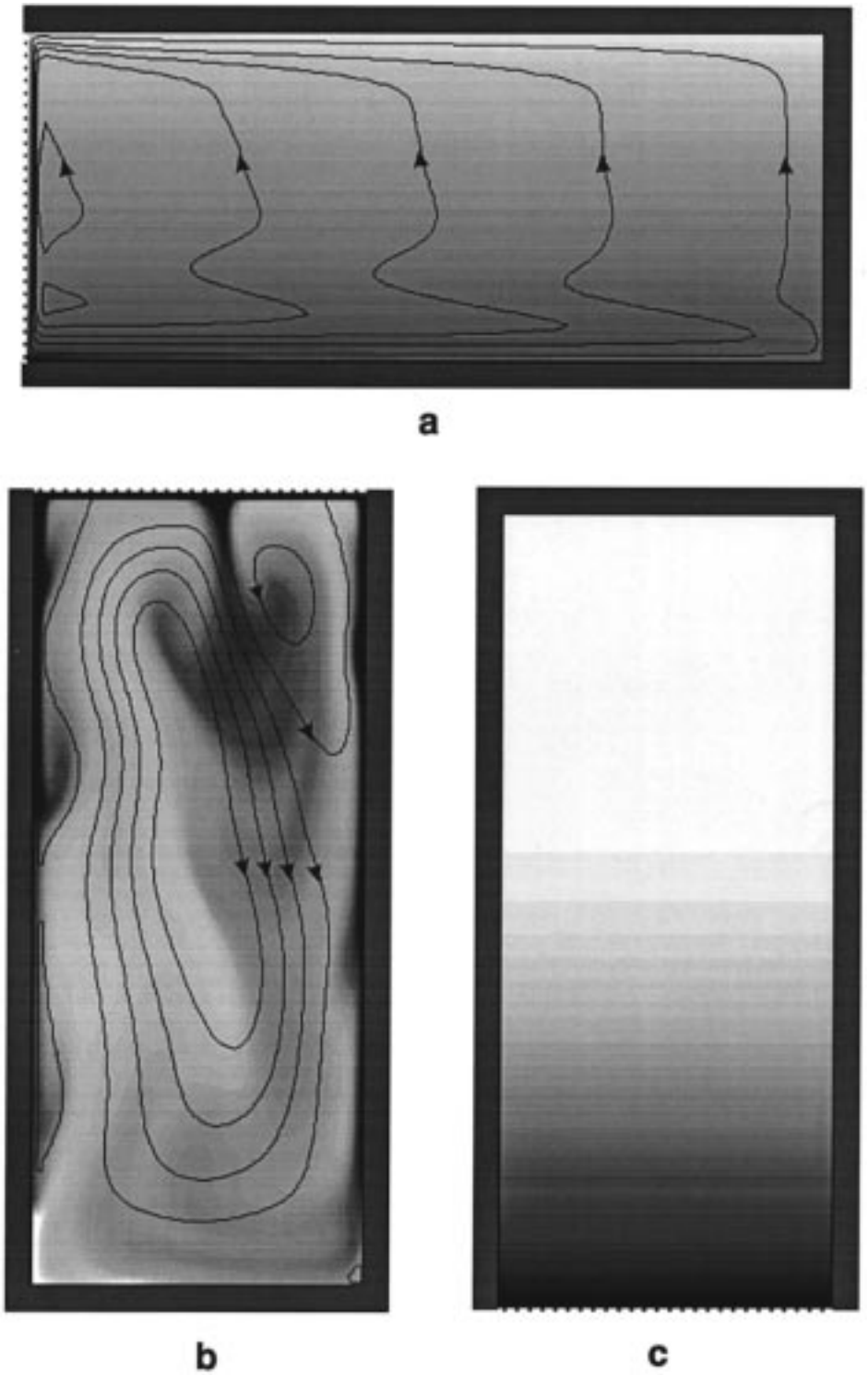

FIGURE 3. Modeled concentration and streamlines within a vial peeper with (a) membrane facing to the left, (b) membrane facing upward, and (c) membrane facing downward. The concentration scale has high concentration dark and low concentration light. The concentration scales differ for the three simulations.

an expression developed by Brandl and Hanselmann (*18*). This solution is obtained from eq 7 with $F = V/A$. In experiment 1, the tank in which the vials were immersed had a sufficiently large volume as compared to the total vial volume and was sufficiently well mixed that the assumption of constant C_0 was considered to be a reasonable one (only 1.5% of the original mass of bromide is removed from the outer tank by diffusion into the vials). Figure 2 compares the results from the instantly mixed model (for $k^m = 3.2 \times 10^{-3}$ mm s^{-1}), the in-cell convection model, and the experimental measurements. Instantly mixed model results are also presented as a shaded region, reflecting the uncertainty in the measured k^m value.

The concentration−time curve generated by the cell convection model provided a reasonable match to the horizontal vial measurements, predicting a slightly shorter equilibration time. However the data are very similar to the instantly mixed model result obtained from eq 8, demonstrating that in-cell convection mixes the cell contents well.

The cell convection model was also used to simulate the equilibration of vials 1−8. The resulting concentration−time curve was almost identical to that created by the simulation for vials 9−17 and is not illustrated. This result would suggest that the equilibration time for vials 1−8 should have been virtually the same as that measured for vials 9−16, but the experiments demonstrated that vials 1−8 equilibrated more slowly. We expect that this difference and the fact that equilibration times are generally underestimated by the instantly mixed model are attributable to boundary layer formation along the membranes in this experiment, which would serve to decrease the effective membrane permeation speed.

Figure 3 shows snapshots of the salt distribution and flow within the cells for three vial orientations: one with the membrane facing vertically upward, one with the membrane facing downward, and the third with the membrane facing horizontally. For the three snapshots, the average salt concentration within the cell is 20% of its equilibrium value. The salt distribution and streamlines in the horizontal vial suggest that the saltwater travels rapidly down the face of the membrane, creating only a thin saltwater layer along this surface. The saline solution moves more slowly along the length of the vial, and cell contents reach equilibrium by a filling process, where the saline layer lying on the horizontal wall gradually thickens (Figure 3a). A very different picture is observed for the vertical vial (Figure 3b). Plumes of saline water plunge down from the membrane surface, and saltwater is also observed to travel down the walls of the vial. As these plumes descend, freshwater is entrained and mixed with the saline solution. The result is that rather than the gradual filling process observed in the horizontal vial, the cell contents are being mixed throughout the equilibration process. When the membrane is facing downward, salt gradually diffuses upward from the membrane uniformly across the width of the vial (Figure 3c).

The predicted ranges of salinities within the vials are quite different for the three vial orientations. For the vial membrane facing upward, the in-cell salinities vary between 7 and 7.5 g L^{-1}, for the sideways facing membrane salinities vary between 2 and 15 g L^{-1}, whereas when the membrane faces downward, in-cell salinities are close to 0 at the top of the vial and close to full salinity (35 g L^{-1}) along the membrane surface.

For the conditions in experiment 1, the instantly mixed model (eq 8) is adequate to estimate the equilibration time for the horizontal vials. If there were no salinity differences and no convection causing mixing within the cell, the instantly mixed model would be inadequate for describing equilibration behavior. A criterion is required to determine the circumstances under which natural convection within the cell is able to mix the cell contents.

Dimensional analysis suggests the following time scales for equilibration in a peeper cell mounted horizontally. We assume the cell has a height h and length (perpendicular to the membrane) l. If diffusion is the only mechanism for transport and the membrane poses no barrier to diffusion, cell equilibration time is expected to scale directly with l^2 and inversely with D. Our numerical simulations suggest the time scale to 90% equilibration is

$$T_d^{90} = 0.8\frac{l^2}{D} \tag{9}$$

Patterson and Imberger (*19*) derived a time scale to reach steady state in a cavity with differentially heated side walls. Their scenario is analogous to our horizontal vial, with the exception that our buoyancy source is salinity rather than heat. The equilibration time scales directly with h and l and inversely with D and $Ra^{1/4}$, where Ra is the cell Rayleigh number:

$$Ra = \frac{g'h^3}{D\nu} \tag{10}$$

where $g' = g\rho/\rho'$ (where ρ is the ambient density and ρ' is the density difference between the water inside and outside the cell at the beginning of the experiment) and ν is the kinematic viscosity. Our numerical simulations suggest the time scale to 90% equilibration in this case is

$$T_c^{90} = 4\frac{hl}{DRa^{1/4}} \tag{11}$$

If the peeper cell is instantly mixed, and equilibration is limited only by the membrane permeation speed, the time to 90% equilibration is calculated from eq 8 as

$$T_m^{90} = 2.3\frac{l}{k^m} \tag{12}$$

Note that for the calculation of T_c^{90}, one needs to set D as the diffusivity of the major species in the outlying medium, which would be NaCl in the case of seawater since it is the major species that causes the convective motions. For computing T_m^{90} and T_d^{90}, D and k^m should assume values appropriate to the particular species of interest.

To estimate the cell equilibration time for a particular peeper configuration one needs to calculate T_m^{90}, T_d^{90}, and T_c^{90}. If $T_d^{90} > T_c^{90}$ then convection is expected to be more effective for mixing the contents of the peeper cell than diffusion and so the mixing time scale for the cell will be T_c^{90}. Similarly, if $T_d^{90} < T_c^{90}$, then the mixing time scale will be T_d^{90}. The lesser of T_d^{90} and T_c^{90} should be compared to T_m^{90} to determine whether cell equilibration is limited primarily by membrane permeation or by cell mixing. Since both membrane permeation and cell mixing limit equilibration, an approximate estimate of the 90% equilibration time is $T_m^{90} + \min(T_d^{90}, T_c^{90})$. Examples of these time scales for various peeper dimensions and salinities are given in Table 1.

TABLE 1. Time Scales for Various Peeper Lengths and Salinities[a]

length (mm)	membrane T_m^{90} (h)	freshwater T_d^{90} (h)	0.1% seawater T_c^{90} (h)	1% seawater T_c^{90} (h)	seawater T_c^{90} (h)
5	1.2	**4**	**2**	1	0.3
10	2.4	**15**	**4**	2	0.6
20	4.7	**59**	**7**	4	1
50	11.8	**370**	**18**	10	3

[a] All calculations assumed a peeper height of 10 mm and a diffusivity of 1.5×10^{-3} mm^2 s^{-1}. T_m^{90} and T_d^{90} do not depend on the salinity, and $T_c^{90} \to \infty$ for freshwater. A boldface value is the most limiting time scale for the corresponding peeper length and salinity. Where T_c^{90} values are not boldface, T_m^{90} is the most limiting time scale for equilibration.

In-Sediment Equilibration Dynamics. The open water diffusivities D were estimated using the analysis of Li and Gregory (*17*) and corrected to a nominal average temperature of 20 °C. From our measurements of membrane permeation speed, we estimated the permeation speed of Na (as a major ion) at 20 °C to be $k^m = 2.7 \times 10^{-3}$ mm s^{-1}. Since the transport of solute through the pores of the membrane is diffusive, we assume that k^m is proportional to D. Then, k^m can be estimated for species other than NaCl as

$$k^m = 2.7 \times 10^{-3}\ \text{mm s}^{-1}\frac{D}{1.5 \times 10^{-3}\ \text{mm}^2\ \text{s}^{-1}} \tag{13}$$

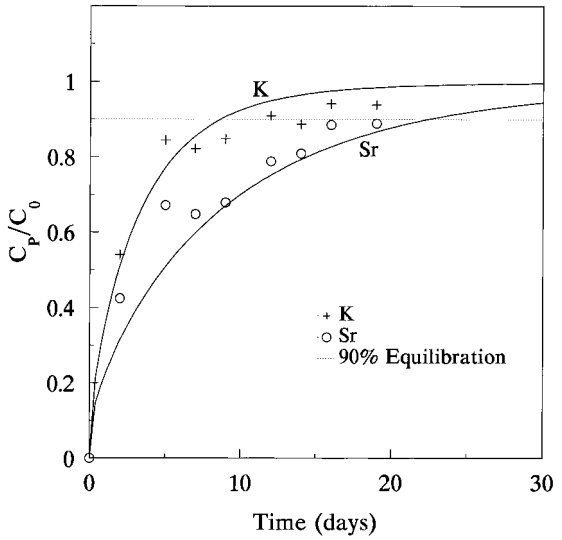

FIGURE 4. Comparison between normalized measurements (symbols) and model predictions for the vial peeper with $F = 15$ mm for K and Sr.

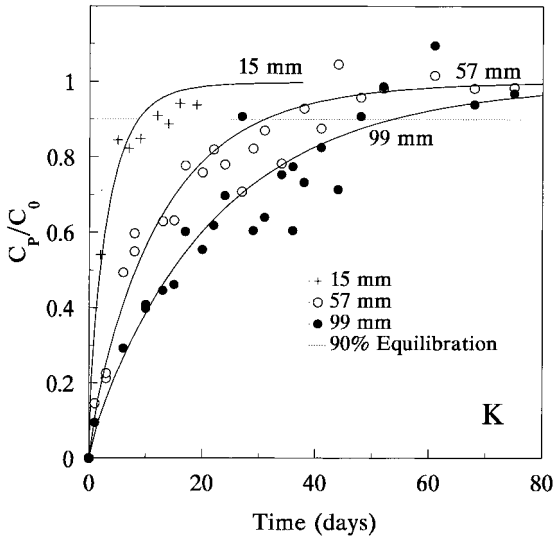

FIGURE 5. Comparison between measurements (symbols) and model predictions (lines) for vial peepers with $F = 15$, 57, and 99 mm for K.

The denominator in this expression is the diffusivity of Na as a major ion at 20 °C.

Boudreau (*20*) considers that the most accurate relationship between porosity and tortuosity is

$$\theta^2 \approx 1 - 2 \ln (\varphi) \qquad (14)$$

This relationship with $\varphi = 0.44$ (the measured porosity) yields $\theta^2 = 2.6$, which is the value we use in our in-sediment equilibration experiments.

Figure 4 compares the measured peeper concentrations to the model predictions for the smallest vial, which has $F = 15$ mm for K and Sr (which have the highest and lowest diffusivities of the four species we investigated). Peeper concentrations have been normalized by the measured pore water concentrations for each case (C_0) so that the equilibration behaviors for the four chemical species can be compared directly. The predicted equilibration rate of the vial concentration increases with the diffusivity of the species being modeled. Potassium, which has $D = 1.9 \times 10^{-3}$ mm^2 s^{-1}, reaches 92% equilibration after 10 days, whereas Sr ($D = 1.9 \times 10^{-3}$ mm^2 s^{-1}) achieves only 70% equilibration after this time. The equilibration curves for Na and Ca (not shown) lie between those for K and Sr.

The predicted concentration curves pass close to all the measurements and are mostly within the 5% expected accuracy of the analytical procedure. The third measurement (at $t = 5$ d) is significantly higher than the predictions for all four species and is higher than the fourth measurement in all cases. Since the cell concentration cannot reduce in time, we suggest that heterogeneity in solute concentrations within the sediment may be responsible for this apparent anomaly. An error in the measured concentration C_0 biases the predictions.

We determined an optimal C_0 by multiplying the simulation with the measured C_0 by a factor that caused the sum of the measured concentrations to equal the sum of the fitted concentrations at the same times. For K, Na, and Ca, the optimal C_0 was 3%, 1%, and 1% lower than the measured C_0; for Sr, the optimal C_0 was 9% higher. The differences between optimal and measured C_0 for K, Na, and Ca are within the analytical uncertainty, whereas for Sr the difference is a little larger. Thus, the measurements support the validity of the in-sediment equilibration model and also demonstrate the dependence of equilibration rate on diffusivity.

Figure 5 compares the model predictions to the measurements for the vial peepers with $F = 15$, 57, and 99 mm for K. Although consecutive measured (normalized) concentrations for the 57 and 99 mm vials vary up and down by about 0.1 or so, they do generally increase toward 1.0 with increasing time. Overall, the rate of approach of measured concentrations toward equilibration decreases with increasing vial design factor in a way that is consistent with model prediction. The predicted times for the peeper to achieve 90% equilibration for K, which has the largest diffusivity of the four species considered, are 9, 30, and 53 days for the 15, 57, and 99 mm peepers, respectively; for Sr, which has the lowest diffusivity, the respective times are 21, 51, and 90 days.

From eq 12, the times for 90% equilibration for the 15, 57, and 99 mm vials, assuming membrane permeation alone limits equilibration, are 3, 11, and 19 h for K and 8, 28, and 49 h for Sr. Furthermore, with the experimental situation of horizontal vials being immersed in seawater, the time scales for equilibration due to convection are approximately 1, 4, and 7 h. These times are much less than the 90% equilibration times for the peepers in sediment, indicating that the prime limitation for equilibration is diffusion through the sediment.

Harper et al. (*7*) considered the equilibration of porewater samplers without resupply from the sediment solid phase (the diffusive case considered in our analysis) and with resupply (the "buffered" case). For the latter case, solute concentrations are maintained at their background levels by resupply through desorption from the solid phase or by some other transport mechanism such as convection. Harper et al. (*7*) suggested that Zn and Cd correspond approximately to this case in freshwater sediments. Substances that adsorb to sediments such as metals have been observed to equilibrate in peepers much more quickly than nonadsorbing species (*6*, *21*). For elements that are buffered, we expect that the limitation to equilibration will be permeation through the membrane or perhaps mixing within the peeper cell if the ionic strength of interstitial waters is low.

Our analysis assumes that the dominant transport mechanism for solutes in sediments is molecular diffusion through the pores. It is well-known that in aquatic sediments solute transport rates can be enhanced greatly by burrowing macrobenthos (*22*, *23*). In environments that are hydrodynamically active, enhanced transport within sediments can also occur due to purely physical processes such as waves and current−obstruction interactions (*24*, *25*). Any such

mechanism that causes solute transport near a peeper window to increase significantly beyond that due to molecular diffusion will also decrease peeper equilibration times. Peeper equilibration due to molecular diffusion acting alone should be considered to be a worst case.

Acknowledgments

We are grateful for funding support from the CSIRO Coastal Zone Program. We thank Graeme Batley, Phillip Ford, and Simon Apte from CSIRO and Mike Harper from Lancaster University for their valuable comments and John Buchanan for assisting with the ICPAES analysis. We also thank three anonymous reviewers for their helpful comments.

Literature Cited

(1) Hesslein, R. H. *Limnol. Oceanogr.* **1976**, *22*, 912−914.
(2) Carignan, R. *Limnol. Oceanogr.* **1984**, *29* (3), 667−670.
(3) Gaillard, J. F.; Jeandel, C.; Michard, G.; Nicolas, E. *Mar. Chem.* **1986**, *18*, 233−247.
(4) Tessier, A.; Carignan, R.; Dubreuil, B.; Rapin, F. *Geochim. Cosmochim. Acta* **1989**, *53*, 1511−1522.
(5) Hare, L.; Carignan, R.; Huerta-Diaz, M. A. *Limnol. Oceanogr.* **1994**, *39*, 1653−1668.
(6) Adler, D. M. M.A. Thesis, Columbia University, 1977.
(7) Harper M. H.; Davison W.; Tych W. *Environ. Sci. Technol.* **1997**, *31* (11), 3110−3119.
(8) Bottomley, E. Z.; Bayly, I. L. *Limnol. Oceanogr.* **1984**, *29*, 671−673.
(9) Kaplan, E.; Banerjee, S.; Ronen, D.; Magaritz, M.; Machlin. A.; Sosnow, M.; Koglin, E. *Ground Water* **1991**, *29*, 191−198.
(10) Freeman, P. R.; Hart, B. T.; McKelvie, I. D. *Geochim. Cosmochim. Acta* **1993**, *282*, 379−388.
(11) Carignan, R.; St-Pierre, S.; Gachter, R. *Limnol. Oceanogr.* **1994**, *39*, 468−474.
(12) Roache, P. J. *Computational Fluid Mechanics*; Hermosa Publishers: Albuquerque, NM, 1982.
(13) Batchelor, G. K. *Fluid Dynamics*; Cambridge University Press: London, 1967.
(14) Gill, A. E. *Atmosphere-Ocean Dynamics*: Academic Press: New York, 1982.
(15) Ullman, W. J.; Aller, R. C. *Limnol. Oceanogr.* **1982**, *27*, 552−556.
(16) Shaw, D. A.; Hanratty, T. J. *Am. Inst. Chem. Eng. J.* **1977**, *23*, 28−37.
(17) Li, Y.-H.; Gregory, S. *Geochim. Cosmochim. Acta* **1974**, *38*, 703−714.
(18) Brandl, H.; Hanselmann, K. W. *Aquat. Sci.* **1991**, *53*, 55−73.
(19) Patterson, J. C.; Imberger, J. *J. Fluid Mech.* **1980**, *100*, 65−86.
(20) Boudreau, B. P. *Geochim. Cosmochim. Acta* **1996**, *60*, 3139−3142.
(21) Carignan, R.; Rapin, F.; Tessier, A. *Geochim. Cosmochim. Acta* **1985**, *49*, 2493−2497.
(22) Aller, R. C. In *Animal-Sediment Relations*; McCall, P. I., Tevesz, M. J. S., Eds.; Plenum: London, 1982; Chapter 2.
(23) Matisoff, G.; Fisher, J. B.; Matis, S. *Hydrobiologia* **1985**, *122*, 19−33.
(24) Savant, S. A.; Reible, D. D.; Thibodeaux, L. J. *Water Resour. Res.* **1987**, *23*, 1763−1768.
(25) Webster, I. T.; Taylor, J. H. *Water Resour. Res.* **1992**, *28*, 109−119.

Received for review September 12, 1997. Revised manuscript received March 2, 1998. Accepted March 6, 1998.

ES970815G